

has a suitable redox potential ( $E^\circ = 0.34$  V), but gives rise only to a stable steady state with low  $[I^-]$ . Other non-oscillatory substrates which we have tested, such as hydrazine and hydroxylamine, seem to yield iodide too rapidly, thereby inhibiting reaction (2) and forcing the system into a steady state of high iodide concentration. Stannous ion, which seems to satisfy both our redox potential and kinetic criteria, does not give oscillation because the formation of the slightly soluble  $\text{SnI}_2$  places a relatively low limit on the iodide concentration that can be attained in the reactor. Substrates which, for kinetic reasons, do not give oscillations in the present conditions, may prove oscillatory in different conditions.

Further studies under way in this laboratory on the detailed mechanism of these systems will hopefully reveal more about the role of the substrate in the family of chlorite-iodate-substrate oscillators.

This work was supported by grant CHE 79-05911 from the NSF.

Received 6 April; accepted 22 June 1981.

1. De Kepper, P., Epstein, I. R. & Kustin, K. *J. Am. chem. Soc.* **103**, 2133-2134 (1981).
2. Bognár, J. & Sárosi, S. *Analyt. chim. Acta* **29**, 406-411 (1963).
3. Eggert, J. & Scharnow, B. *Z. Electrochem.* **27**, 455-470 (1927).
4. Kern, D. M. & Kim, C.-H. *J. Am. chem. Soc.* **87**, 5309-5313 (1965).
5. de Meus, J. & Sigalla, J. *J. chim. Phys.* **63**, 453-459 (1966).
6. Dateo, C., Orbán, M., De Kepper, P. & Epstein, I. R. *J. Am. chem. Soc.* (in the press).
7. Boissonade, J. & De Kepper, P. *J. phys. Chem.* **84**, 501-506 (1980).
8. Latimer, W. M. *Oxidation Potentials* 2nd edn (Prentice Hall, Englewood Cliffs, 1964).
9. Clark, W. M. *Oxidation-Reduction Potential of Organic Systems*, 470 (Williams and Wilkins, Baltimore, 1960).

## Crystal structure of tetrapropylammonium fluoride-silicalite

G. D. Price, J. J. Pluth, J. V. Smith & T. Araki

Department of the Geophysical Sciences, University of Chicago, Chicago, Illinois 60637, USA

J. M. Bennett

Union Carbide Corporation, Tarrytown, New York 10591, USA

The hydrophobic and organophilic nature<sup>1</sup> of silicalite may prove commercially important for the removal of organic compounds from waste water. The framework linkage of silicalite<sup>1</sup> is topologically the same as that of synthetic zeolite ZSM-5 (ref. 2), a shape-selective catalyst<sup>3</sup> capable of converting methanol into water and hydrocarbons useful in automobile engines<sup>4</sup>. The tetrapropylammonium (TPA) fluoride (F)-containing precursor to fluoride-silicate<sup>5</sup> crystallizes from a hydrothermal system containing silica,  $\text{TPA}^+$  and  $\text{F}^-$  ions. Destruction of the organic cation during heating in air gives fluoride-silicalite, a polymorph of silica with some properties similar to those of silicalite<sup>1,5</sup>. We show here how a TPAF complex in the precursor lies at the tetrahedral intersection of the 10-ring channels of a silica framework in a position consistent with a template scheme for crystallization<sup>6</sup>. There is not enough space to permit replacement of TPA by the tetra-*n*-butyl ammonium complex used in the synthesis of ZSM-11 (ref. 7) and its silica counterpart, silicalite-2 (ref. 8)

Crystals of the precursor are interpenetrant twins elongated along the *c*-axis ( $180 \times 50 \times 50$   $\mu\text{m}$ ). The twin boundaries are  $\{110\}$  and the twin law is  $90^\circ$  rotation about  $[001]$ . Single-crystal X-ray and optical studies yielded monoclinic symmetry ( $a$ , 20.04;  $b$ , 19.92;  $c$ , 13.39 Å;  $\beta \sim 90^\circ$ ). Because of the near-equivalence of the  $a$  and  $b$  axial lengths, the twinning causes near-superposition of  $hkl$  and  $khl$  diffractions. The intensities of over 12,000 diffractions, each an  $hkl$ ,  $khl$  pair, were measured over one quadrant of reciprocal space (MoK $\alpha$  radiation) using a four-circle diffractometer. In spite of the optically monoclinic symmetry, the intensities are consistent with orthorhombic space group Pnma used for the refinement of silicalite<sup>9</sup>. The following structure description uses this space group and an

orthorhombic cell with the above cell dimensions. Averaged intensities for 1,645 unique diffractions with  $F_{\text{obs}} > 2\sigma$  allowed refinement of the silica framework to  $R = 0.10$  with a special least-squares program TWXLLS. The combined intensity of  $pI(khl) + (1-p)I(hkl)$  for a pseudo-tetragonal twin was split into the individual intensities  $I(hkl)$  and  $I(khl)$  for the pseudo-orthorhombic structure where the fractional volume  $p$  of one twin component was refined from all the intensities. A difference-Fourier synthesis revealed one organic complex at each of the four intersections of the 10-ring channels (Fig. 1), corresponding to a unit cell composition of 4 TPAF.96 SiO<sub>2</sub>. Least-squares refinement yielded  $R = 0.07$  and the atomic coordinates in Table 1. The coordinates of the silica framework are similar to those for silicalite<sup>9</sup>. Because of the restricted data set and some disorder of the TPAF complex, individual isotropic displacement factors were used for the framework atoms and a single displacement factor for the TPAF. No significant electron density was found in a difference-Fourier map based on the coordinates of Table 1.

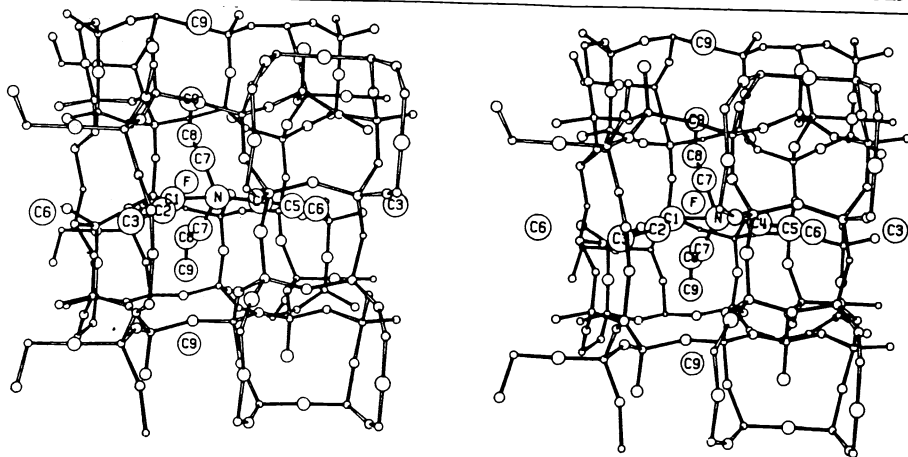
The silica framework has a mean Si-O bond length of 1.60 Å ( $\sigma$  0.04) and a range of Si-O-Si angles of  $136$ - $178^\circ$  about a

Table 1 Atomic coordinates for the fluoride silicalite precursor

Atom	x	y	z
Si(1)	0.1213	0.3255	0.9729
Si(2)	0.2741	0.3252	0.9712
Si(3)	0.0768	0.4410	0.8364
Si(4)	0.0712	0.3692	0.1828
Si(5)	0.3144	0.4403	0.8319
Si(6)	0.3080	0.3711	0.1879
Si(7)	0.0733	0.5271	0.1868
Si(8)	0.3080	0.5296	0.1926
Si(9)	0.3127	0.6736	0.8214
Si(10)	0.2799	0.5600	0.9709
Si(11)	0.1227	0.5635	0.9716
Si(12)	0.0762	0.6712	0.8279
O(1)	0.1137	0.2500	0.9287
O(2)	0.1957	0.3464	0.9619
O(3)	0.0825	0.3711	0.8876
O(4)	0.0933	0.3374	0.0843
O(5)	0.2915	0.2500	0.9450
O(6)	0.3155	0.3704	0.8917
O(7)	0.3095	0.3496	0.0732
O(8)	0.9955	0.5423	0.2139
O(9)	0.3702	0.5543	0.2460
O(10)	0.0865	0.5019	0.9174
O(11)	0.0817	0.4514	0.1766
O(12)	0.1150	0.3392	0.2656
O(13)	0.9973	0.3471	0.2054
O(14)	0.3856	0.4432	0.7808
O(15)	0.2564	0.4359	0.7459
O(16)	0.2940	0.4977	0.9096
O(17)	0.3090	0.4481	0.1925
O(18)	0.2547	0.6501	0.7496
O(19)	0.3749	0.3396	0.2391
O(20)	0.0986	0.5612	0.0853
O(21)	0.3070	0.5618	0.0839
O(22)	0.3029	0.7500	0.8487
O(23)	0.3128	0.6299	0.9202
O(24)	0.2036	0.5608	0.9696
O(25)	0.0990	0.6324	0.9269
O(26)	0.0724	0.7500	0.8610
N	0.4478	0.7500	0.1036
C(1)	0.5347	0.7500	0.1373
C(2)	0.5791	0.7500	0.2595
C(3)	0.6115	0.7500	0.3780
C(4)	0.3583	0.7500	0.1430
C(5)	0.3217	0.7500	0.1792
C(6)	0.2586	0.7500	0.1921
C(7)	0.4821	0.6487	0.0649
C(8)	0.5067	0.6454	0.9911
C(9)	0.5023	0.5688	0.9842
F	0.5059	0.7500	0.9366

Standard deviations for Si, O and non-framework atoms are  $\sim 0.0006$ , 0.001 and 0.005 respectively.

**Fig. 1** Stereoview of TPA-F complex and adjacent atoms from the silica framework. ORTEP plot with spheres at 20% probability level.



mean of  $153.6^\circ$  ( $\sigma$  11.4). A negative correlation between Si-O bond lengths and secant (Si-O-Si) for the 4-coordinated silica polymorphs<sup>10</sup> was interpreted in terms of overlap of molecular orbitals. The present structure shows a similar relationship with slope 0.13 (correlation coefficient 0.6), close to that predicted theoretically for a silica cluster in Fig. 8a of ref. 11.

The tetrahedral configuration of the four propyl limbs of the TPA ion and the close coordination of the fluoride to the central nitrogen at 2.52 Å and four carbons all at 2.21 Å is physically reasonable and resembles that in the crystal structure of TPA-bromide<sup>12</sup>. Two propyl limbs partly envelop the fluoride, and a fifth carbon atom from a third limb lies at 2.75 Å to the fluorine atom. Because hydrogen bonds involving F<sup>-</sup> span a range<sup>13</sup> of 2.3–2.8 Å which almost encompasses the above distances, the fluoride ion is probably held in place by hydrogen bonding.

The neat fit between the TPAF complex and the internal surface of the silica framework is consistent with a template mechanism for crystallization<sup>6</sup>. Furthermore, the end carbon atom of each propyl limb lies at 2.8–3.1 Å to the end carbon atom of the propyl limb from the next TPAF complex, and there would not be enough space for a butyl limb. Although there are no published atomic coordinates for the structures of ZSM-11 (ref. 7) or its silica counterpart, silicalite-2 (ref. 8) which can be synthesized from tetra-*n*-butylammonium-containing systems, models with plausible geometry show that the channel intersections are larger than for the ZSM-5 and silicalite type of linkage, and in particular are large enough for a butyl-bearing complex. Knowledge of the structural interactions between tetrahedral frameworks and occluded complexes should prove useful in designing conditions for crystallization of useful shape-selective catalysts.

Further data are being collected to increase the precision of the atomic coordinates. The cause of the monoclinic symmetry is also being investigated. The present study has indirect implications for various inorganic-organic complexes, including ones involving clays<sup>14</sup> and biologically important compounds.

We thank R. L. Patton for providing the crystal. We thank NSF for grant CHE 78-26579, and R. Draus and I. Baltuska for technical assistance. T. A. thanks P. B. Moore for NSF grant EAR 19483. X-ray facilities are partly supported by the Materials Research Laboratory (NSF).

Received 23 April; accepted 9 July 1981.

1. Flanigen, E. M. *et al.* *Nature* **271**, 512–516 (1978).
2. Kokotailo, G. T., Lawton, S. L., Olson, D. H. & Meier, W. M. *Nature* **272**, 437–438 (1978).
3. Kokotailo, G. T. & Meier, W. M. *Chem. Soc. Spec. Publ.* **33**, 133–139 (1980).
4. Meisel, S. L., McCullough, J. P., Lechthaler, C. H. & Weisz, P. B. *Chem. Technol.* **6**, 86 (1976).
5. Flanigen, E. M. & Patton, R. L. US Patent NM 4073865 (1978).
6. Flanigen, E. M. *Adv. Chem. Ser.* **121**, 119–139 (1973).
7. Kokotailo, G. T., Chu, P., Lawton, S. L. & Meier, W. M. *Nature* **275**, 119–120 (1978).
8. Bibby, D. M., Milestone, N. B. & Aldridge, L. P. *Nature* **280**, 664–665 (1979).
9. Smith, J. V. *Discuss. 5th Int. Conf. on Zeolites* (in the press).
10. Meagher, E. P., Tossell, J. A. & Gibbs, G. V. *Phys. Chem. Miner.* **4**, 11–21 (1979).
11. Newton, M. D. & Gibbs, G. V. *Phys. Chem. Miner.* **6**, 221–246 (1980).
12. Zalkin, A. *Acta Crystallogr.* **10**, 557–560 (1957).
13. Durrant, P. J. & Durrant, B. *Advanced Inorganic Chemistry* (Wiley, New York, 1964).
14. Theng, B. K. G. *Formation and Properties of Clay-Polymer Complexes* (Elsevier, Amsterdam, 1979).

## Dehydration-induced luminescence in clay minerals

L. M. Coyne, N. Lahav & J. G. Lawless

Ames Research Center, NASA, Moffett Field, California 94035, USA

Reports of triboluminescent phenomena in organic crystalline materials<sup>1,2</sup> prompted us to look for related processes in clay minerals. We found the reported extensive mechanical distortion produced on freezing and drying of montmorillonite<sup>3</sup> particularly interesting because of our studies of condensation reactions in a wet/dry cycled reaction sequence<sup>4–7</sup>. We now report the discovery of an unusual luminescent process in several clay minerals and describe its characteristics.

We have found that blue to near UV photons are emitted when a thin layer of an aqueous suspension of certain clays is dried over a desiccant or by gentle heating to 85 °C (ref. 7). Figure 1a–c shows typical examples of three distinctive patterns of photon release as a function of time. The patterns are: (1) a delayed burst, (2) a delayed rise to a slowly decaying plateau and (3) a simple monotonic (exponential-like) decay from the time of introduction of the desiccant.

Kaolinites show an initial monotonically decaying emission of photons followed, some minutes to hours later, by the delayed burst. Two examples are shown in Fig. 1a, Fisher kaolinite and Mesa Alta rock, ground in a mortar and pestle a few days before sample preparation. A similar pattern of emission was observed from all other kaolinites examined; Peerless no. 2; kaolin no. 53 from Birch Pit, Macon, Georgia, and kaolin no. 17 from Lewis-town, Missouri. The photon yield and relative proportion of monotonic to delayed emission varied from kaolinite to kaolinite. The time of onset of the burst is increased by a thicker film. The light is released when the average moisture content approaches 40% H<sub>2</sub>O. The significance of this moisture content with respect to water content at the drying front is uncertain, but the average range is within the quoted range for the adsorption and long-range ordering of water by kaolin<sup>8</sup>. Multiple peaks are frequently observed, especially in the non-commercial kaolinites; the peaks seem to be largely, but not fully, explained as experimental artefacts resulting from non-uniformity in the thickness of the clay film and the size of the particles.

The amount of light released on dehydration is an approximately linear function of the amount of kaolin, up to a film thickness of ~10 μm (as calculated from the dry weight of kaolin, the exposed surface area of the emitting film and its estimated density), after which self-absorption and scattering produce a gradual saturation<sup>7</sup>. Light release can be regenerated by repeated cycles of wetting and drying, up to at least four cycles, or until deterioration of the clay film prevents further trials.